JOURNAL OF SPACECRAFT AND ROCKETS
Vol. 35, No. 3, May–June 1998

Low-Thrust Eccentricity-Constrained Orbit Raising

Jean Albert Kechichian*
The Aerospace Corporation, El Segundo, California 90245-4691

The problem of zero-eccentricity-constrained orbit raising in circular orbit in the presence of shadowing is analyzed using both numerical and analytical methods. Given the shadow arclength, piecewise constant pitch angles are selected analytically, and the location along the orbit where the pitch angle switches is optimized to effect the largest change in semimajor axis per revolution. Two strategies yielding near-optimal performance are presented, differing in whether or not a pitch reorientation maneuver is carried out inside the shadow arc. These analytic results are also compared with the exact eccentricity-constrained numerical solutions, which use optimally varying continuous pitch profiles to maximize the change in semimajor axis after each revolution. The suboptimal analytic strategies are almost as effective as the optimal strategy especially in higher orbit. These strategies remove the need for continuously reorienting the spacecraft attitude in pitch, providing robust real-time on-board guidance capability for electric orbit transfer vehicle orbit raising applications.

Nomenclature

a_0, a = initial and current orbit semimajor axis, km
c_θ, s_θ = $\cos\theta$, $\sin\theta$, etc.
e_0, e = initial and current orbit eccentricity
f_r, f_θ = components of acceleration vector along radial and perpendicular directions
f_t, f_n = components of acceleration vector along tangential and normal directions
h = orbital angular momentum, $[\mu a(1-e^2)]^{1/2}$
k = thrust acceleration, T/m, km/s^2
m = spacecraft mass, kg
n = orbit mean motion, $(\mu/a_0^3)^{1/2}$
p = orbit parameter, $a(1-e^2)$, km
r = radial distance, $p(1+ec_{\theta^*})^{-1}$, km
$\boldsymbol{T}$ = thrust vector
v = orbital velocity on circular orbit, na_0
δ = shadow angle
θ = angular position of spacecraft measured from x axis
θ_t = thrust vector pitch angle
θ_t', θ_t'' = pitch angle before and after switch point, respectively
θ^* = true anomaly
μ = Earth gravity constant, 398,601.3, km^3/s^2
τ = nondimensional time, nt
τ_c = angular position of switch point measured from x axis
τ_1, τ_2 = angular position of shadow entry and exit points
ω = argument of perigee

Introduction

THE general problem of circle-to-circle transfer with inclination change using continuous constant acceleration has been solved analytically by Edelbaum.[1] The assumption of a constant yaw profile within each revolution, adopted by Edelbaum, has been removed by Wiesel and Alfano,[2] who optimized the yaw profile by also allowing the continuous acceleration magnitude to vary due to propellant expenditure. Semianalytic solutions of the optimal thrust pitch and yaw profiles for a given transfer were determined by Cass[3] and McCann,[4] who also generalized the problem further by considering discontinuous thrust due to eclipsing. In Ref. 5, a computer program that simulates the important effects due to shadowing or eclipsing and power degradation during transit in the Van Allen radiation belts has been created. The intermediate orbits during the transfer are assumed to remain circular by Dickey et al.[5] to simplify the calculations of the orbit parameters as well as the shadow entry and exit points, even though exact numerical simulations for typical six-month solar-electric transfers from low Earth orbit (LEO) to geostationary Earth orbit show that in the worst case of shadowing geometry the intermediate orbits could reach eccentricities on the order of 0.2 at most. Analytic solutions for the inclination control and orbit raising when shadowing is present are depicted[6,7] for implementation in efficient codes such as in the case of Ref. 5. In view of the small eccentricity buildup, it is convenient to force eccentricity to remain at zero by developing analytic methods that result in simple but suboptimal steering laws that are easily implementable in mission analysis software and by fully accounting for the varying shadow geometry during the transfer. Thus, orbit raising in the presence of shadowing, which can be difficult to model in LEO, remains complicated if the orbit must be constrained to remain circular during the coplanar transfer. The main advantage of keeping the eccentricity at zero during the transfer is that it simplifies the equations of motion to their simplest form, which then allows the analyst to carry out the optimization problem semianalytically as in Ref. 3. Another important advantage consists in the ease of computing the shadow entry and exit points because they are given in analytic form instead of numerically solving a quartic that would be computationally intensive and therefore may not be of interest for on-board navigation applications. Unlike the approach of Ref. 3, we consider constant relative pitch angles that are easily implemented by the on-board attitude control system, which in this case has to hold the pitch attitude constant relative to the local horizon. The adoption of piecewise constant pitch angles allows the spacecraft to pitch at the same rate as the orbital motion, thereby removing the need to continuously maneuver in attitude as in Ref. 3, where an optimal variable pitch profile is implemented instead.

Our approach is based on the theory of function minimization and is purely analytic, requiring minimal computational effort. In the second section, we consider that no pitch attitude maneuvers should be implemented in shadow when sun sensors are ineffective (strategy 1). The strategy of the third section is free of such requirements (strategy 2), and in both cases the optimal switch location is found such that the largest change in semimajor axis is achieved during one revolution of intermittent thrusting. We shall also seek constant pitch angle solutions over a large portion of the sunlit arc such that unique combinations of the pitch angles for a given switch location along the orbit result in a net zero eccentricity buildup, albeit with a correspondingly degraded semimajor axis buildup when compared with the optimal switch location solution.

Analysis

Let x, y represent an Earth-centered inertial reference frame such that y bisects the shadow arc O′O as in Fig. 1. The shadow entry

Presented as Paper 91-156 at the AAS/AIAA Spaceflight Mechanics Meeting, Houston, TX, Feb. 11–13, 1991; received May 23, 1997; revision received Feb. 16, 1998; accepted for publication Feb. 16, 1998.

*Engineering Specialist, Astrodynamics Department, MS M4/947, P.O. Box 92957, Los Angeles, CA 90009. E-mail: Jean.A.Kechichian@aero.org. Associate Fellow AIAA.

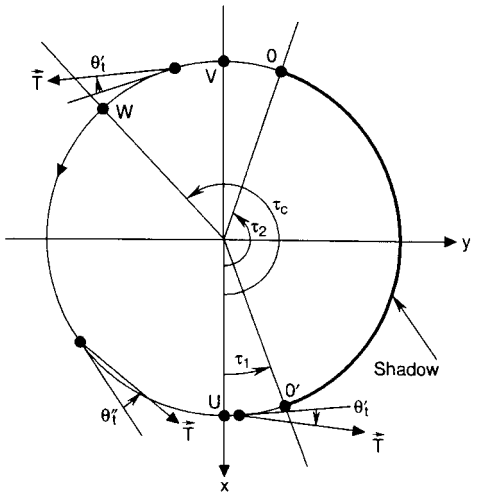

Fig. 1 Orbit geometry.

point is O′, and the shadow exit point is O. The location of O′ is measured from the x axis by the angle τ_1, and due to symmetry, the angular position of O is depicted by $\tau_2 = \pi - \tau_1$. Thrust is applied only when the spacecraft is in sunlight, and time is measured from the x axis. In a first analysis, and starting from point U at time zero, a constant acceleration thrust $\boldsymbol{T}$ is applied along the arc UO′ such that the thrust vector is inclined at a constant angle θ_t' with respect to the local horizontal. This simple scheme is easily implemented by the attitude control system of the spacecraft because the vehicle is continuously pitching at the same rate as the orbital mean motion. Furthermore, to prevent any attitude control maneuvers while in shadow, the same constant angle θ_t' is maintained at the exit from the shadow along the arc OVW. At the W location, the thrust angle is switched from θ_t' to θ_t'' and held at this constant value from W to U, completing, thereby, one full revolution. This switch point W is defined by τ_c. The angle τ_1 is always in the first quadrant because the maximum shadow angle $\delta = \tau_2 - \tau_1$ never exceeds 140 deg, which, of course, takes place in LEO. The orbit is in full sunlight if $\tau_2 = \tau_1 = \pi/2$. This problem is best analyzed by making use of the variation of parameters perturbation equations linearized about a reference circular orbit, which we will consider to be the initial circular orbit at time zero. We seek solutions for θ_t', θ_t'', and τ_c such that after each revolution of the Earth the orbit remains circular with no buildup in eccentricity and while thrusting only in sunlight. Because we are interested only in the coplanar problem, the equations that describe the perturbations of the semimajor axis a and the eccentricity vector $\boldsymbol{e}$ are given by

$$\frac{\mathrm{d}\Delta a}{\mathrm{d}\tau} = \frac{2a_0^3}{\mu} f_\theta \tag{1}$$

$$\frac{\mathrm{d}\Delta e_x}{\mathrm{d}\tau} = \frac{a_0^2}{\mu}(2c_\theta f_\theta + s_\theta f_r) \tag{2}$$

$$\frac{\mathrm{d}\Delta e_y}{\mathrm{d}\tau} = \frac{a_0^2}{\mu}(2s_\theta f_\theta - c_\theta f_r) \tag{3}$$

The rates are with respect to τ. The vector $\boldsymbol{e}$ has been replaced by its components e_x and e_y along the inertial x and y directions such that there are no singularities at $e = 0$ with the use of this formulation. From $\Delta a = a - a_0$ and using the variation of parameters equation $\dot{a} = (2a_0^2/\mu)vf_t$, where $v = na_0$ and $f_t = f_\theta$ for a circular orbit, the rate in Eq. (1) is obtained from $\mathrm{d}\Delta a/\mathrm{d}t = (2a_0^3/\mu)nf_\theta$. Similarly, from $\Delta e_x = e_x - e_{x_0} = ec_\omega - e_0 c_{\omega_0}$ and $\mathrm{d}\Delta e_x/\mathrm{d}t = \dot{e}c_\omega - es_\omega\dot{\omega}$, letting $\omega = 0$, and using the variation of parameters equation for the eccentricity,[8]

$$\dot{e} = (r/h)\left[s_{\theta^*}(1 + ec_{\theta^*})f_r + \left(e + 2c_{\theta^*} + ec_{\theta^*}^2\right)f_\theta\right]$$

with $r = a_0$, $h = (\mu a_0)^{1/2}$, $\theta^* = \theta - \omega$ with $\omega = 0$, and letting $e = 0$, the rate in Eq. (2) is obtained. Finally, from $\Delta e_y = e_y - e_{y0}$, $\mathrm{d}\Delta e_y/\mathrm{d}t = \dot{e}s_\omega + ec_\omega\dot{\omega}$, where[8]

$$e\dot{\omega} = (r/h)[-c_{\theta^*}(1 + ec_{\theta^*})f_r + s_{\theta^*}(2 + ec_{\theta^*})f_\theta]$$

and making the same substitutions as for the Δe_x case, Eq. (3) is obtained. Let k represent the magnitude of the constant acceleration imparted to the spacecraft; m is updated if needed from orbit to orbit. Then

$$f_r = ks_{\theta_t} \tag{4}$$

$$f_\theta = kc_{\theta_t} \tag{5}$$

Then, because the orbit is to remain circular at the end of each revolution, and near circular in between, $\theta \cong nt = \tau$ is used in Eqs. (1–3), yielding

$$\frac{\mathrm{d}\Delta a}{\mathrm{d}\tau} = \frac{2}{n^2}kc_{\theta_t} \tag{6}$$

$$\frac{\mathrm{d}\Delta e_x}{\mathrm{d}\tau} = \frac{k}{a_0 n^2}\left(2c_{\theta_t}c_\tau + s_{\theta_t}s_\tau\right) \tag{7}$$

$$\frac{\mathrm{d}\Delta e_y}{\mathrm{d}\tau} = \frac{k}{a_0 n^2}\left(2c_{\theta_t}s_\tau - s_{\theta_t}c_\tau\right) \tag{8}$$

Let us examine first the case of pure tangential thrust where $\theta_t = 0$. Then the preceding system of equations is integrated between 0 and τ_1 and between τ_2 and 2π and, after adding, yields the changes in a, e_x, and e_y, namely, $\Delta a = (2k/n^2)(\tau_1 - \tau_2 + 2\pi)$, $\Delta e_x = (2k/a_0 n^2)(s_{\tau_1} - s_{\tau_2})$, and $\Delta e_y = -(2k/a_0 n^2)(c_{\tau_1} - c_{\tau_2})$. These expressions show that Δe_x and Δe_y are equal to zero only for $\tau_1 = \tau_2$, which takes place if $\tau_1 = \pi/2$, i.e., the case of no shadow. It is therefore impossible to thrust tangentially along the velocity vector without building up net eccentricity. In fact, in view of $\tau_2 = \pi - \tau_1$, the preceding expressions reduce to $\Delta a = (2k/n^2)(\pi + 2\tau_1)$, $\Delta e_x = 0$, and $\Delta e_y = (-4k/a_0 n^2)c_{\tau_1}$, with $\Delta a > 0$ and $\Delta e_y \le 0$, because τ_1 is always such that $0 < \tau_1 \le \pi/2$. If we integrate the equations of motion with $\theta_t = \theta_t'$ for $0 \le \tau \le \tau_1$ and $\tau_2 \le \tau \le \tau_c$ and $\theta_t = \theta_t''$ for $\tau_c \le \tau \le 2\pi$, then

$$\Delta a = (2k/n^2)\left[(\tau_1 + \tau_c - \tau_2)c_{\theta_t'} + (2\pi - \tau_c)c_{\theta_t''}\right] \tag{9}$$

$$\Delta e_x = \left(k/a_0 n^2\right)\left[2\left(s_{\tau_1} + s_{\tau_c} - s_{\tau_2}\right)c_{\theta_t'} - 2s_{\tau_c}c_{\theta_t''} - \left(c_{\tau_1} - c_{\tau_2} - 1 + c_{\tau_c}\right)s_{\theta_t'} - \left(1 - c_{\tau_c}\right)s_{\theta_t''}\right] \tag{10}$$

$$\Delta e_y = -\left(k/a_0 n^2\right)\left[2\left(c_{\tau_1} - 1 + c_{\tau_c} - c_{\tau_2}\right)c_{\theta_t'} + 2\left(1 - c_{\tau_c}\right)c_{\theta_t''} + \left(s_{\tau_1} + s_{\tau_c} - s_{\tau_2}\right)s_{\theta_t'} - s_{\tau_c}s_{\theta_t''}\right] \tag{11}$$

Let us consider purely tangential acceleration-deceleration programs. If we choose $\theta_t' = \pi$ and $\theta_t'' = 0$, then we have a deceleration-acceleration program such that the preceding expressions reduce to

$$\Delta a = (2k/n^2)(3\pi - 2\tau_c - 2\tau_1) \tag{12}$$

$$\Delta e_x = -\left(4k/a_0 n^2\right)s_{\tau_c} \tag{13}$$

$$\Delta e_y = \left(4k/a_0 n^2\right)\left(c_{\tau_1} + c_{\tau_c} - 1\right) \tag{14}$$

It is seen here that $\Delta e_x = 0$ if $\tau_c = \pi, 2\pi$. For $\tau_c = \pi$, $\Delta e_y = 0$ if $c_{\tau_1} - 2 = 0$, which is clearly impossible. For $\tau_c = 2\pi$, Δe_y vanishes only if $c_{\tau_1} = 0$ or $\tau_1 = \pi/2$, indicating the case of no shadow. Therefore, this deceleration-acceleration program cannot yield Δe_x and $\Delta e_y = 0$ simultaneously as long as there is a shadow arc along the orbit.

For $\tau_1 = \pi/2$ and $\tau_c = 2\pi$, we have $\Delta a = -4\pi k/n^2 < 0$, which would shrink the orbit. The same discussion will hold true if we consider an acceleration-deceleration program with $\theta_t' = 0$ and $\theta_t'' = \pi$. In this case, Eqs. (9–11) yield the exact negative expressions of Eqs. (12–14). In these expressions, $\Delta e_x = 0$ for $\tau_c = \pi$ or 2π. If $\tau_c = \pi$, $\Delta e_y = 0$ requires $2 - c_{\tau_1} = 0$, which is impossible, and if $\tau_c = 2\pi$, the condition $\Delta e_y = 0$ requires $c_{\tau_1} = 0$ or $\tau_1 = \pi/2$, where no shadow arc exists. In this case, $\Delta a = 4\pi k/n^2 > 0$, which is strictly positive as expected. If one uses the first strategy (deceleration-acceleration) during one orbit and the second strategy

(acceleration-deceleration) during the following orbit or vice versa, it is possible to keep $\Delta e_y = 0$ if τ_c is selected such that $c_{\tau_c} = 1 - c_{\tau_1}$. The Δe_x change from the first revolution will cancel out the Δe_x change from the following revolution so that both Δe_x and Δe_y will remain at zero after each two orbits. However, this strategy will also yield a net Δa of zero, which is not desirable. Let us consider one final strategy in which $\theta_t = \theta_t'$ for $0 \le \tau \le \tau_1$, $\theta_t = \theta_t''$ for $\tau_2 \le \tau \le \tau_c$, and $\theta_t = \theta_t'''$ for $\tau_c \le \tau \le 2\pi$. Then the integration of the linearized differential equations will yield

$$\Delta a = (2k/n^2)\left[\tau_1 c_{\theta_t'} + (\tau_c - \tau_2) c_{\theta_t''} + (2\pi - \tau_c) c_{\theta_t'''}\right] \tag{15}$$

$$\Delta e_x = \left(k/a_0 n^2\right)\left[2 s_{\tau_1} c_{\theta_t'} + \left(1 - c_{\tau_1}\right) s_{\theta_t'} + 2\left(s_{\tau_c} - s_{\tau_2}\right) c_{\theta_t''} - \left(c_{\tau_c} - c_{\tau_2}\right) s_{\theta_t''} - 2 s_{\tau_c} c_{\theta_t'''} - \left(1 - c_{\tau_c}\right) s_{\theta_t'''}\right] \tag{16}$$

$$\Delta e_y = -\left(k/a_0 n^2\right)\left[-2\left(1 - c_{\tau_1}\right) c_{\theta_t'} + s_{\tau_1} s_{\theta_t'} + 2\left(c_{\tau_c} - c_{\tau_2}\right) c_{\theta_t''} + \left(s_{\tau_c} - s_{\tau_2}\right) s_{\theta_t''} + 2\left(1 - c_{\tau_c}\right) c_{\theta_t'''} - s_{\tau_c} s_{\theta_t'''}\right] \tag{17}$$

If we consider now an acceleration-deceleration-acceleration program with $\theta_t' = 0$, $\theta_t'' = \pi$, and $\theta_t''' = 0$, then the preceding equations reduce to

$$\Delta a = (2k/n^2)(3\pi - 2\tau_c) \tag{18}$$

$$\Delta e_x = \left(4k/a_0 n^2\right)\left(s_{\tau_1} - s_{\tau_c}\right) \tag{19}$$

$$\Delta e_y = \left(4k/a_0 n^2\right) c_{\tau_c} \tag{20}$$

Clearly, both Δe_x and Δe_y cannot be equal to zero regardless of the value of τ_c because $\Delta e_x = 0$ for $\tau_c = \pi - \tau_1 = \tau_2$ and $\Delta e_y = 0$ for $\tau_c = 3\pi/2$. In a similar manner, if we consider now a deceleration-acceleration-deceleration program with $\theta_t' = \pi$, $\theta_t'' = 0$, and $\theta_t''' = \pi$, then the variations are opposite in sign to Eqs. (18–20), and for the same reason, it is impossible to satisfy $\Delta e_x = \Delta e_y = 0$ simultaneously. From these simple examples, it is seen that purely tangential thrusting in the presence of shadow arcs will not satisfy the $e = 0$ constraint. Therefore, we must investigate strategies with $\theta_t \neq 0$ such that we can control the eccentricity buildup through the radial components of the acceleration vectors when shadowing is present. Going back to Eqs. (9–11), the conditions $\Delta e_x = 0$ and $\Delta e_y = 0$ yield the system of equations given by

$$2A c_{\theta_t'} - B s_{\theta_t'} - 2C c_{\theta_t''} - D s_{\theta_t''} = 0 \tag{21}$$

$$2B c_{\theta_t'} + A s_{\theta_t'} + 2D c_{\theta_t''} - C s_{\theta_t''} = 0 \tag{22}$$

with $A = s_{\tau_1} - s_{\tau_2} + s_{\tau_c} = s_{\tau_c}$, $B = c_{\tau_1} - c_{\tau_2} - 1 + c_{\tau_c} = 2c_{\tau_1} - 1 + c_{\tau_c}$, $C = s_{\tau_c}$, and $D = 1 - c_{\tau_c}$. For given τ_1 and τ_c, Eqs. (21) and (22) can be solved to give $s_{\theta_t''}$ and $c_{\theta_t''}$ in terms of $s_{\theta_t'}$ and $c_{\theta_t'}$

$$s_{\theta_t''} = \frac{2(AD + BC) c_{\theta_t'} + (AC - BD) s_{\theta_t'}}{(C^2 + D^2)}$$

$$c_{\theta_t''} = \frac{2(AC - BD) c_{\theta_t'} - (BC + AD) s_{\theta_t'}}{2(C^2 + D^2)}$$

However, from the preceding definitions, $B + D = 2c_{\tau_1}$, $A^2 + D^2 = C^2 + D^2 = 2D = 2(1 - c_{\tau_c})$, and $A^2 - BD = 2(1 - c_{\tau_c})(1 - c_{\tau_1})$ such that

$$s_{\theta_t''} = \frac{2 s_{\tau_c} c_{\tau_1} c_{\theta_t'} + \left(1 - c_{\tau_c}\right)\left(1 - c_{\tau_1}\right) s_{\theta_t'}}{\left(1 - c_{\tau_c}\right)} \tag{23}$$

$$c_{\theta_t''} = \frac{2\left(1 - c_{\tau_1}\right)\left(1 - c_{\tau_c}\right) c_{\theta_t'} - s_{\tau_c} c_{\tau_1} s_{\theta_t'}}{2\left(1 - c_{\tau_c}\right)} \tag{24}$$

These expressions will be useful when we evaluate θ_t'' once θ_t' is known. Let us now rewrite Eqs. (9–11) as

$$\Delta a = (2k/n^2)\left[(\tau_c + 2\tau_1 - \pi) c_{\theta_t'} + (2\pi - \tau_c) c_{\theta_t''}\right] \tag{25}$$

$$\Delta e_x = \left(k/a_0 n^2\right)\left[2 s_{\tau_c} c_{\theta_t'} - \left(2c_{\tau_1} - 1 + c_{\tau_c}\right) s_{\theta_t'} - 2 s_{\tau_c} c_{\theta_t''} - \left(1 - c_{\tau_c}\right) s_{\theta_t''}\right] \tag{26}$$

$$\Delta e_y = -\left(k/a_0 n^2\right)\left[2\left(2c_{\tau_1} - 1 + c_{\tau_c}\right) c_{\theta_t'} + s_{\tau_c} s_{\theta_t'} + 2\left(1 - c_{\tau_c}\right) c_{\theta_t''} - s_{\tau_c} s_{\theta_t''}\right] \tag{27}$$

The last two expressions can be written in terms of $s_{\theta_t'}$ and $s_{\theta_t''}$, and because we require $\Delta e_x = \Delta e_y = 0$, they reduce to

$$2 s_{\tau_c}(\pm)\left(1 - s_{\theta_t'}^2\right)^{\frac{1}{2}} - \left(2c_{\tau_1} - 1 + c_{\tau_c}\right) s_{\theta_t'} - 2 s_{\tau_c}(\pm)\left(1 - s_{\theta_t''}^2\right)^{\frac{1}{2}} - \left(1 - c_{\tau_c}\right) s_{\theta_t''} = 0 \tag{28}$$

$$2\left(2c_{\tau_1} - 1 + c_{\tau_c}\right)(\pm)\left(1 - s_{\theta_t'}^2\right)^{\frac{1}{2}} + s_{\tau_c} s_{\theta_t'} + 2\left(1 - c_{\tau_c}\right)(\pm)\left(1 - s_{\theta_t''}^2\right)^{\frac{1}{2}} - s_{\tau_c} s_{\theta_t''} = 0 \tag{29}$$

From Eqs. (28) and (29)

$$s_{\theta_t''} = \frac{2 s_{\tau_c} c_{\tau_1}(\pm)\left(1 - s_{\theta_t'}^2\right)^{\frac{1}{2}} + \left(1 - c_{\tau_c}\right)\left(1 - c_{\tau_1}\right) s_{\theta_t'}}{\left(1 - c_{\tau_c}\right)} \tag{30}$$

If we square this expression for $s_{\theta_t''}$ and replace in Eq. (28), we get after regrouping terms

$$\pm\left(1 - s_{\theta_t'}^2\right)^{\frac{1}{2}} K_1 - s_{\theta_t'} K_2 = \pm 2 s_{\tau_c}\left(1 - s_{\theta_t''}^2\right)^{\frac{1}{2}} \tag{31}$$

where the right-hand side term is written in terms of Eq. (30) and where $K_1 = 2s_{\tau_c}(1 - c_{\tau_1})$ and $K_2 = c_{\tau_1}(1 + c_{\tau_c})$. Squaring Eq. (31) once more yields

$$L_1 + s_{\theta_t'}^2 L_2 = \pm s_{\theta_t'}\left(1 - s_{\theta_t'}^2\right)^{\frac{1}{2}} L_3 \tag{32}$$

with

$$L_1 = 4 s_{\tau_c}^2 c_{\tau_1}\left[\left(c_{\tau_1} - 2\right) + \frac{4 s_{\tau_c}^2 c_{\tau_1}}{\left(1 - c_{\tau_c}\right)^2}\right] \tag{33}$$

$$L_2 = -15 c_{\tau_1}^2\left(1 + c_{\tau_c}\right)^2 \tag{34}$$

$$L_3 = \frac{-12 s_{\tau_1}^3 c_{\tau_1}\left(1 - c_{\tau_1}\right)}{\left(1 - c_{\tau_c}\right)} \tag{35}$$

The term L_1 can also be written as

$$L_1 = 4\left(1 + c_{\tau_c}\right) c_{\tau_1}\left[c_{\tau_c}\left(3c_{\tau_1} + 2\right) + \left(5c_{\tau_1} - 2\right)\right] \tag{36}$$

We square Eq. (32) once again to get an expression in $s_{\theta_t'}$

$$s_{\theta_t'}^4\left(L_2^2 + L_3^2\right) + \left(2L_1 L_2 - L_3^2\right) s_{\theta_t'}^2 + L_1^2 = 0$$

The preceding expression being a quadratic in $s_{\theta_t'}^2$, its solutions are given by

$$s_{\theta_t'}^2 = \frac{-2\left(L_1 L_2 - L_3^2\right) \pm \left[\left(2L_1 L_2 - L_3^2\right)^2 - 4\left(L_2^2 + L_3^2\right) L_1^2\right]^{\frac{1}{2}}}{2\left(L_2^2 + L_3^2\right)} = (S_1, S_2) \tag{37}$$

where S_1 corresponds to the plus sign and S_2 to the minus sign in Eq. (37). Therefore, the angle θ_t' is such that

$$s_{\theta_t'} = \pm(S_1)^{\frac{1}{2}}, \qquad \pm(S_2)^{\frac{1}{2}} \tag{38}$$

providing no fewer than eight solutions due to the double squaring operations just carried out. Four of these solutions can be eliminated if we require that $c_{\theta_t'} > 0$ or $-\pi/2 \le \theta_t' \le \pi/2$ so that the $c_{\theta_t'}$ term in the Δa expression in Eq. (25) contributes to a positive Δa for orbit raising. From Eq. (25), $(\tau_1 - \tau_2 + \tau_c) > 0$ and $(\tau_c - 2\pi) < 0$ so that $\Delta a > 0$ would require $c_{\theta_t'}(\tau_1 + \tau_c - \tau_2) > -c_{\theta_t''}(2\pi - \tau_c)$. If $c_{\theta_t'} < 0$, then we must have $c_{\theta_t''} > 0$, and to have $\Delta a > 0$, we must additionally satisfy $|c_{\theta_t''}(2\pi - \tau_c)| > |c_{\theta_t'}(\tau_1 + \tau_c - \tau_2)|$, which requires, in turn, that

$$\tau_c < \frac{2\pi\left|c_{\theta_t''}\right| + (\tau_2 - \tau_1)\left|c_{\theta_t'}\right|}{\left|c_{\theta_t'}\right| + \left|c_{\theta_t''}\right|}$$

If $c_{\theta_t'} > 0$, then $c_{\theta_t''} > 0$ always satisfies the inequality $c_{\theta_t'}(\tau_1 + \tau_c - \tau_2) > -c_{\theta_t''}(2\pi - \tau_c)$, and $\Delta a > 0$ is always satisfied. However, if $c_{\theta_t''} < 0$, then $\Delta a > 0$ requires the satisfaction of $|c_{\theta_t'}(\tau_1 + \tau_c - \tau_2)| > |c_{\theta_t''}(2\pi - \tau_c)|$, which is possible for

$$\tau_c > \frac{2\pi\left|c_{\theta_t''}\right| + (\tau_2 - \tau_1)\left|c_{\theta_t'}\right|}{\left|c_{\theta_t'}\right| + \left|c_{\theta_t''}\right|}$$

Let us consider only accelerating solutions of the type $c_{\theta_t'}$ and $c_{\theta_t''} > 0$. Equation (34) for L_2 is such that $L_2 < 0$ is always satisfied for any τ_1 and τ_c. The expression for L_3 in Eq. (35) is such that

$$L_3 \le 0 \quad \text{if} \quad \tau_2 < \tau_c \le \pi \quad \text{or} \quad s_{\tau_c} \ge 0$$

$$L_3 \ge 0 \quad \text{if} \quad \pi \le \tau_c \le 2\pi \quad \text{or} \quad s_{\tau_c} \le 0$$

From Eq. (36), it is seen that $L_1 > 0$ if $c_{\tau_c} > (2 - 5c_{\tau_1})/(2 + 3c_{\tau_1})$ because $(1 + c_{\tau_c})$ and c_{τ_1} are always positive. Furthermore, $\tau_c \ge \tau_2$ must hold, such that $L_1 < 0$ for $\tau_2 \le \tau_c < \tau_c'$, where τ_c' is obtained from

$$c_{\tau_c'} = \frac{(2 - 5c_{\tau_1})}{(2 + 3c_{\tau_1})} \tag{39}$$

At $\tau_c = \tau_c'$, $L_1 = 0$, and for $\tau_c' < \tau \le 2\pi$, $L_1 > 0$. From Eq. (37), it is clear that $(2L_1L_2 - L_3^2)$ must be negative because $4(L_2^2 + L_3^2)L_1^2 \ge 0$ and $L_2^2 + L_3^2 \ge 0$; otherwise $s_{\theta_t'}^2$ would be negative, which is impossible. Therefore

$$M_1 = 2L_1L_2 - L_3^2 < 0 \tag{40}$$

Replacing from Eqs. (34–36), this inequality reduces to $M_1 = -24(1 + c_{\tau_c})^3 c_{\tau_1}^2 [c_{\tau_c}(9c_{\tau_1}^2 + 22c_{\tau_1} - 6) + (31c_{\tau_1}^2 - 22c_{\tau_1} + 6)] < 0$, which, in view of the minus sign and the fact that $(1 + c_{\tau_c})^3 c_{\tau_1}^2 > 0$ is always satisfied, translates to the condition

$$c_{\tau_c}\left(9c_{\tau_1}^2 + 22c_{\tau_1} - 6\right) + \left(31c_{\tau_1}^2 - 22c_{\tau_1} + 6\right) > 0 \tag{41}$$

For a given τ_1, this inequality is satisfied if τ_c is such that

$$c_{\tau_c} > \frac{\left(-31c_{\tau_1}^2 + 22c_{\tau_1} - 6\right)}{\left(9c_{\tau_1}^2 + 22c_{\tau_1} - 6\right)} \tag{42}$$

The quadratic functions appearing in Eq. (41) are plotted in Fig. 2. At $\tau_1 = 70.985$ deg, they intersect, and Eq. (42) becomes $c_{\tau_c} > -1$, which is satisfied for every τ_c. The values of τ_c, which are the switch points that satisfy Eq. (41) or $M_1 < 0$, are shown in Figs. 3 and 4 for various values of τ_1. For $\tau_1 = 0$ deg, $M_1 < 0$ is satisfied if 233.13 deg $< \tau_c \le 2\pi$. This case of maximum shadow angle $\tau_2 - \tau_1 = \pi$ is for an orbit with zero altitude. For Earth orbiters in LEO, τ_1 is always larger than 20 deg, and the locus of τ_c that satisfies $M_1 < 0$ is given by 215.27 deg $< \tau_c \le 2\pi$. The switch points are, of course, obtained from

$$c_{\tau_c} = \frac{-31c_{\tau_1}^2 + 22c_{\tau_1} - 6}{9c_{\tau_1}^2 + 22c_{\tau_1} - 6} \tag{43}$$

with the additional condition that $\tau_c \ge \tau_2$. Figure 4 shows that as we approach $\tau_1 = 70.98$ deg, there are two regions along the orbit for which $M_1 < 0$ is satisfied; these two regions eventually merge such that for $\tau_1 > 70.98$ deg all values of $\tau_c \ge \tau_2$ satisfy $M_1 < 0$. Another condition that the switch point τ_c must satisfy is given by

$$\left(2L_1L_2 - L_3^2\right)^2 - 4\left(L_2^2 + L_3^2\right)L_1^2 \ge 0 \tag{44}$$

The preceding equation is the discriminant in Eq. (37), and its satisfaction ensures that the roots $s_{\theta_t'}^2$ do indeed exist. This condition is equivalent to

$$L_3^2 - 4L_1(L_1 + L_2) \ge 0 \tag{45}$$

and because from Eqs. (34–36)

$$L_1 + L_2 = c_{\tau_1}\left(1 + c_{\tau_c}\right)\left[c_{\tau_1}\left(5 - 3c_{\tau_c}\right) - 8\left(1 - c_{\tau_c}\right)\right]$$

the condition in Eq. (45) is reduced, after some algebraic manipulations, to the following quadratic form in c_{τ_c}:

$$N_2 = -25c_{\tau_c}^2 + 32\left(1 - c_{\tau_1}\right)c_{\tau_c} - \left[7 + 16c_{\tau_1}\left(c_{\tau_1} - 2\right)\right] \ge 0 \tag{46}$$

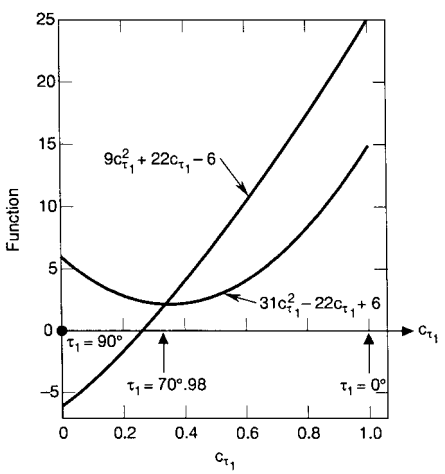

Fig. 2 Switch point conditions for full range of shadow entry angle.

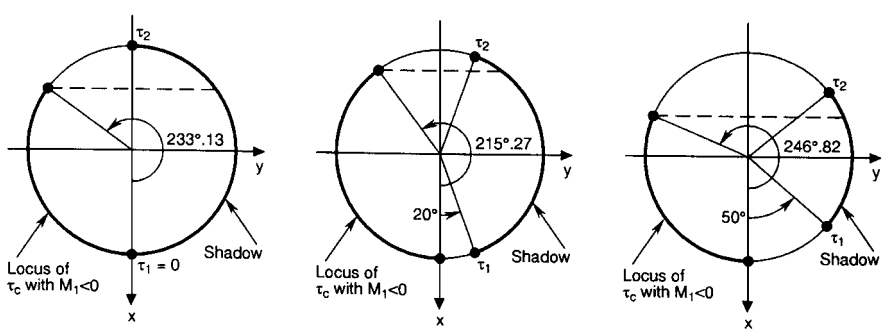

Fig. 3 Feasible regions for τ_c satisfying the $M_1 < 0$ condition for three values of $\tau_1 = 0$, 20, and 50 deg.

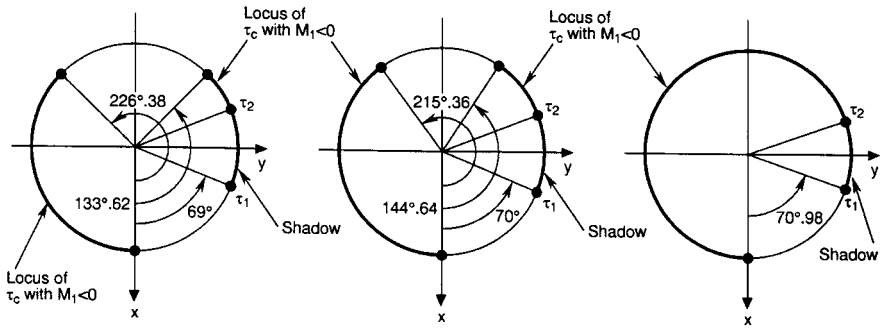

Fig. 4 Feasible regions for τ_c satisfying the $M_1 < 0$ condition for larger values of $\tau_1 = 69$, 70, and 70.98 deg.

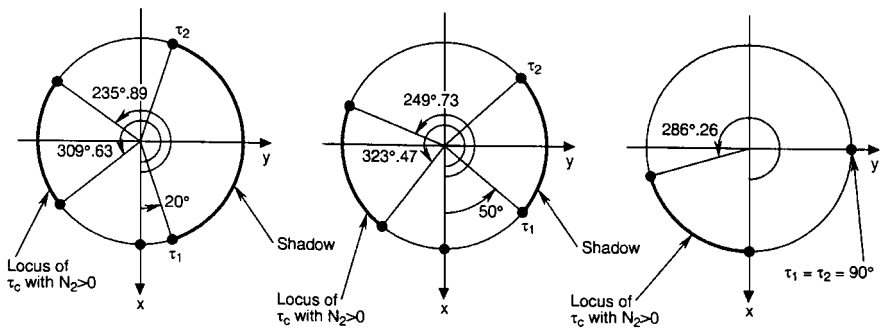

Fig. 5 Feasible regions for τ_c satisfying the $N_2 > 0$ condition for $\tau_1 = 20$, 50, and 90 deg.

whose roots are given by

$$c_{\tau_c} = \frac{16\left(1 - c_{\tau_1}\right) \pm \left(-144c_{\tau_1}^2 + 288c_{\tau_1} + 81\right)^{\frac{1}{2}}}{25} \tag{47}$$

Here, the discriminant is positive semidefinite for $c_{\tau_1} \geq -0.250$ so that for $0 \leq \tau_1 \leq 90$ it always holds, and therefore c_{τ_c} always exists. In fact, the condition in Eq. (46) is always satisfied by τ_c for which c_{τ_c} is between the two roots of Eq. (47). This condition is shown in Fig. 5 for three values of τ_1, namely, $\tau_1 = 20$, 50, and 90 deg. As τ_1 varies, the τ_c arc for which $N_2 > 0$ maintains a constant length of 73.74 deg while shifting toward the x axis, which is reached for $\tau_1 = 90$ deg. Because both conditions $M_1 < 0$ and $N_2 > 0$ must be satisfied by τ_c for any given τ_1, the intersection of the two regions defines the locus of feasible τ_c. It is found that the $N_2 > 0$ region is always contained in the larger $M_1 < 0$ region, with the lower boundaries being as close as 0.1 deg to one another for $\tau_1 = 24$ deg. Therefore, the satisfaction of $N_2 > 0$ guarantees the satisfaction of $M_1 < 0$ for all $0 \leq \tau_1 \leq 90$ deg of interest. Now, the same manipulations that lead to the generation of Eq. (32) can be repeated to obtain an expression in terms of $c_{\theta_t'}$ instead of $s_{\theta_t'}$. Without going through the details of the derivations, we can obtain an expression for $s_{\theta_t''}$ from Eqs. (26) and (27) identical to Eq. (30), except that $s_{\theta_t''}$ is now expressed in terms of $c_{\theta_t'}$ instead of $s_{\theta_t'}$ as in Eq. (30). Squaring that expression results in

$$L_0 - L_2 c_{\theta_t'}^2 = \pm c_{\theta_t'}\left(1 - c_{\theta_t'}^2\right)^{\frac{1}{2}} L_3 \tag{48}$$

with L_0 given by

$$L_0 = 4s_{\tau_c}^2 c_{\tau_1}\left(c_{\tau_1} - 2\right) + c_{\tau_1}^2\left(1 + c_{\tau_c}\right)^2 \tag{49}$$

and with L_2 and L_3 as before in Eqs. (34) and (35), respectively. Equation (46) reduces, after squaring and replacement, to the form

$$c_{\theta_t'}^4\left(L_2^2 + L_3^2\right) + \left(-2L_0L_2 - L_3^2\right)c_{\theta_t'}^2 + L_0^2 = 0$$

whose solutions are given by

$$c_{\theta_t'}^2 = \frac{-\left(-2L_0L_2 - L_3^2\right) \pm \left[\left(-2L_0L_2 - L_3^2\right)^2 - 4\left(L_2^2 + L_3^2\right)L_0^2\right]^{\frac{1}{2}}}{2\left(L_2^2 + L_3^2\right)} \tag{50}$$

Letting $M_2 = L_2^2 + L_3^2$ and $M_3 = -2L_0L_2 - L_3^2$, then

$$c_{\theta_t'}^2 = \frac{-M_3 + \left(M_3^2 - 4M_2L_0^2\right)^{\frac{1}{2}}}{2M_2} = S_3$$

$$c_{\theta_t'}^2 = \frac{-M_3 - \left(M_3^2 - 4M_2L_0^2\right)^{\frac{1}{2}}}{2M_2} = S_4$$

so that finally the solutions reduce to

$$c_{\theta_t'} = \pm(S_3)^{\frac{1}{2}} \tag{51}$$

$$c_{\theta_t'} = \pm(S_4)^{\frac{1}{2}} \tag{52}$$

It is easily verified that $L_0 = L_1 + L_2$, where L_1 is as given in Eq. (36). We could have also obtained $c_{\theta_t'}^2$ directly from $c_{\theta_t'}^2 = 1 - s_{\theta_t'}^2$ such that

$$c_{\theta_t'}^2 = \frac{\left(2L_1L_2 + 2L_2^2 + L_3^2\right) \mp \left[\left(2L_1L_2 - L_3^2\right)^2 - 4\left(L_2^2 + L_3^2\right)L_1^2\right]^{\frac{1}{2}}}{2\left(L_2^2 + L_3^2\right)}$$

We get the following four solutions for the thrust angle θ_t' by observing that from Eqs. (38), (51), and (52) the S_1 solution for $s_{\theta_t'}$ corresponds to the S_4 solution for $c_{\theta_t'}$, and similarly for S_2 and S_3, such that the four solutions that satisfy $\Delta e = 0$ are given by

$$\theta_t' = \tan^{-1}\left[\frac{(S_1)^{\frac{1}{2}}}{-(S_4)^{\frac{1}{2}}}\right] \tag{53}$$

$$\theta_t' = \tan^{-1}\left[\frac{-(S_1)^{\frac{1}{2}}}{(S_4)^{\frac{1}{2}}}\right] \tag{54}$$

$$\theta_t' = \tan^{-1}\left[\frac{(S_2)^{\frac{1}{2}}}{(S_3)^{\frac{1}{2}}}\right] \tag{55}$$

$$\theta_t' = \tan^{-1}\left[\frac{-(S_2)^{\frac{1}{2}}}{-(S_3)^{\frac{1}{2}}}\right] \tag{56}$$

We could also have obtained from $\Delta e_x = \Delta e_y = 0$ of Eqs. (26) and (27) an expression for $c_{\theta_t''}$ in terms of $c_{\theta_t'}$ that would have led to

$$L_1' + c_{\theta_t'}^2 L_2' = \pm c_{\theta_t'}\left(1 - c_{\theta_t'}^2\right)^{\frac{1}{2}} L_3'$$

which, when squared, yields the quadratic form in $c_{\theta_t'}^2$

$$c_{\theta_t'}^4\left(L_2'^2 + L_3'^2\right) + \left(2L_1'L_2' - L_3'^2\right)c_{\theta_t'}^2 + L_1'^2 = 0$$

whose solutions are given by

$$c_{\theta_t'}^2 = \frac{-M_1' \pm \left(M_1'^2 - 4M_2'L_1'^2\right)^{\frac{1}{2}}}{2M_2'} \tag{57}$$

where

$$M_1' = 2L_1'L_2' - L_3'^2, \qquad M_2' = L_2'^2 + L_3'^2$$

$$L_1' = \frac{\left(1 + c_{\tau_c}\right)c_{\tau_1}}{4}\left[5c_{\tau_1} - 3c_{\tau_1}c_{\tau_c} - 8\left(1 - c_{\tau_c}\right)\right]$$

$$L_2' = \frac{15}{4}c_{\tau_1}^2\left(1 + c_{\tau_c}\right)^2 = \frac{-L_2}{4}$$

$$L_3' = 3s_{\tau_c}c_{\tau_1}\left(1 + c_{\tau_c}\right)\left(1 - c_{\tau_1}\right) = \frac{-L_3}{4}$$

The solutions are given by

$$c_{\theta_t'} = \pm(S_3')^{\frac{1}{2}}, \qquad c_{\theta_t'} = \pm(S_4')^{\frac{1}{2}} \tag{58}$$

with S_3' corresponding to the plus sign in Eq. (57) and S_4' to the minus sign, respectively. We can also write the solutions for θ_t' in terms S_1, S_2, S_3', and S_4' as

$$\theta_t' = \tan^{-1}\left[\frac{(S_1)^{\frac{1}{2}}}{-(S_4')^{\frac{1}{2}}}\right] \tag{59}$$

$$\theta_t' = \tan^{-1}\left[\frac{-(S_1)^{\frac{1}{2}}}{(S_4')^{\frac{1}{2}}}\right] \tag{60}$$

$$\theta_t' = \tan^{-1}\left[\frac{(S_2)^{\frac{1}{2}}}{(S_3')^{\frac{1}{2}}}\right] \tag{61}$$

$$\theta_t' = \tan^{-1}\left[\frac{-(S_2)^{\frac{1}{2}}}{-(S_3')^{\frac{1}{2}}}\right] \tag{62}$$

Once the four solutions are found for θ_t', the solutions for θ_t'' are obtained from Eqs. (23) and (24), which express $s_{\theta_t''}$ and $c_{\theta_t''}$, respectively, in terms of θ_t'. Next, Δa in kilometers and Δe_x and Δe_y are also evaluated from Eqs. (25–27). It is thus found that the preceding four solutions are symmetrical two by two, meaning that two solutions provide positive Δa and the other two mirror values of Δa but with $\Delta a < 0$. The $\Delta a > 0$ solutions are to be used for orbit raising, whereas the $\Delta a < 0$ solutions will be used for the return leg to LEO. The obvious choice is, of course, the solution that provides the largest Δa whether positive or negative. The solution given in Eq. (61) provides the largest $\Delta a > 0$, and the solution given in Eq. (62) provides the largest $\Delta a < 0$. Let a_0 =40,000 km, μ =398,601.3 km^3/s^2, $k = 3.5 \times 10^{-7}$ km/s^2, and $\tau_1 = 80$ deg. Starting from $\tau_c = \tau_2 = \pi - \tau_1 = 100$ deg, Δa, Δe_x, and Δe_y are evaluated from Eqs. (25–27) after computing the four solutions θ_t' that satisfy $\Delta e_x = \Delta e_y = 0$ from Eqs. (59–62) and evaluating the corresponding angles θ_t'' from Eqs. (23) and (24). For Each τ_c, the discriminants in Eqs. (44), (50), and (57) are evaluated to determine whether they are positive or negative. If they are negative, then no solution is possible, and a larger τ_c is selected until they are positive. Once this condition is satisfied, the four θ_t' angles are computed, followed by the four corresponding θ_t'' values.

Initially, only the first two solutions satisfy $\Delta e_x = \Delta e_y = 0$, and as τ_c is increased further, all four solutions are acceptable, whereas the last τ_c value used in this example will result in the satisfaction of only the last two solutions. Clearly there exists a value of τ_c for which Δa is maximum, which, in this case, is about 640 km. It is very easy to mechanize this algorithm and step on τ_c one degree at a time, or less if so desired, and select the solution that provides the largest Δa using a search and sort routine. Incidentally, only those values of τ_c that satisfy the condition $N_2 > 0$ of Fig. 5 produce any feasible solutions as expected.

Modified Strategy for Eccentricity Control

In this analysis, the x axis is along the shadow exit point as indicated by point O in Fig. 6. The thrust $\boldsymbol{T} = \boldsymbol{f}$ is again applied at a constant pitch angle θ_t' with respect to the local horizon from shadow exit to point W defined by the angle τ_c. At this point, the pitch angle is changed to the constant value of θ_t'' until shadow entry defined by point O′, where thrust is interrupted until shadow exit.

This strategy requires, unlike the strategy of the second section, that the vehicle perform an attitude adjust maneuver in shadow so that the pitch angle θ_t' is recovered at exit for another revolution of intermittent low thrust around Earth. In this analysis, the shadow entry point O′ is defined by the angular position of τ_f, and the shadow arc length is defined by the angle $\delta = 2\alpha$ such that $\tau_f = 2\pi - \delta$. Going back to the linearized perturbation Eqs. (6–8) and integrating between 0 and τ_c with the pitch angle of θ_t', and then from τ_c to τ_f with θ_t'', we obtain

$$\Delta a = (2k/n^2)\left[c_{\theta_t'}\tau_c + c_{\theta_t''}(\tau_f - \tau_c)\right] \tag{63}$$

$$\Delta e_x = \left(k/a_0n^2\right)\left[2c_{\theta_t'}s_{\tau_c} + s_{\theta_t'}\left(1 - c_{\tau_c}\right) + 2c_{\theta_t''}\left(s_{\tau_f} - s_{\tau_c}\right) - s_{\theta_t''}\left(c_{\tau_f} - c_{\tau_c}\right)\right] \tag{64}$$

$$\Delta e_y = -\left(k/a_0n^2\right)\left[-2c_{\theta_t'}\left(1 - c_{\tau_c}\right) + s_{\theta_t'}s_{\tau_c} + 2c_{\theta_t''}\left(c_{\tau_f} - c_{\tau_c}\right) + s_{\theta_t''}\left(s_{\tau_f} - s_{\tau_c}\right)\right] \tag{65}$$

Once again, we require $\Delta e_x = \Delta e_y = 0$ such that from Eqs. (64) and (65) expressions for $s_{\theta_t''}$ and $c_{\theta_t''}$ in terms of $s_{\theta_t'}$ and $c_{\theta_t'}$ can be obtained:

$$s_{\theta_t''} = \frac{2(A'D' + B'C')c_{\theta_t'} + (B'D' - A'C')s_{\theta_t'}}{(C'^2 + D'^2)} \tag{66}$$

$$c_{\theta_t''} = \frac{2(B'D' - A'C')c_{\theta_t'} - (B'C' + A'D')s_{\theta_t'}}{2(C'^2 + D'^2)} \tag{67}$$

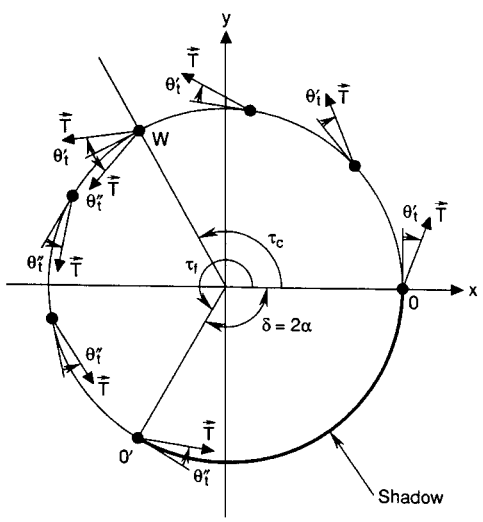

Fig. 6 Transfer geometry with pitch reorientation maneuver in shadow.

where

$$A' = s_{\tau_c}, \qquad B' = 1 - c_{\tau_c}$$

$$C' = s_{\tau_f} - s_{\tau_c}, \qquad D' = c_{\tau_f} - c_{\tau_c}$$

and where

$$A'D' + B'C' = s_{\tau_f}\left(1 - c_{\tau_c}\right) - s_{\tau_c}\left(1 - c_{\tau_f}\right)$$

$$(C'^2 + D'^2) = 2\left[1 - s_{\tau_c}s_{\tau_f} - c_{\tau_c}c_{\tau_f}\right]$$

$$B'D' - A'C' = 1 + c_{\tau_f} - c_{\tau_c} - s_{\tau_f}s_{\tau_c} - c_{\tau_f}c_{\tau_c}$$

To solve for the pitch angle θ_t', Eqs. (64) and (65) are written in terms of the sine functions only:

$$\pm 2\left(1 - s_{\theta_t'}^2\right)^{\frac{1}{2}} A' + s_{\theta_t'}B' \pm 2\left(1 - s_{\theta_t''}^2\right)^{\frac{1}{2}} C' - s_{\theta_t''}D' = 0 \quad (68)$$

$$-(\pm)2\left(1 - s_{\theta_t'}^2\right)^{\frac{1}{2}} B' + s_{\theta_t'}A' \pm 2\left(1 - s_{\theta_t''}^2\right)^{\frac{1}{2}} D' + s_{\theta_t''}C' = 0 \quad (69)$$

Let us solve for $s_{\theta_t''}$ in terms of $s_{\theta_t'}$ from the preceding two expressions. Then

$$s_{\theta_t''} = \frac{\pm 2(A'D' + B'C')\left(1 - s_{\theta_t'}^2\right)^{\frac{1}{2}} - (A'C' - B'D')s_{\theta_t'}}{(C'^2 + D'^2)}$$

If we replace this expression back in Eq. (68) and square the resulting expression, we get

$$L_1'' + s_{\theta_t'}^2 L_2'' = -s_{\theta_t'}(\pm)\left(1 - s_{\theta_t'}^2\right)^{\frac{1}{2}} L_3''$$

which is squared one more time to yield the quadratic form in $s_{\theta_t'}^2$

$$s_{\theta_t'}^4\left(L_2''^2 + L_3''^2\right) + \left(2L_1''L_2'' - L_3''^2\right)s_{\theta_t'}^2 + L_1''^2 = 0 \quad (70)$$

with

$$L_1'' = K_1'^2 - 4C'^2 + \frac{16C'^2(A'D' + B'C')^2}{(C'^2 + D'^2)^2}$$

$$L_2'' = K_2'^2 - K_1'^2 - \frac{4C'^2}{(C'^2 + D'^2)^2}[4(A'D' + B'C')^2 - (A'C' - B'D')^2]$$

$$L_3'' = 2K_1'K_2' - \frac{16C'^2}{(C'^2 + D'^2)^2}(A'D' + B'C')(A'C' - B'D')$$

$$K_1' = 2\left[A' - \frac{D'(A'D' + B'C')}{(C'^2 + D'^2)}\right]$$

$$K_2' = B' + \frac{D'(A'C' - B'D')}{(C'^2 + D'^2)}$$

The solutions of Eq. (70) are given by

$$s_{\theta_t'}^2 = \frac{-M_1'' \pm \left(M_1''^2 - 4M_2''L_1''^2\right)^{\frac{1}{2}}}{2M_2''} = (S_1, S_2) \quad (71)$$

such that

$$s_{\theta_t'} = \pm(S_1)^{\frac{1}{2}} \quad (72)$$

$$s_{\theta_t'} = \pm(S_2)^{\frac{1}{2}} \quad (73)$$

with S_1 corresponding to the plus sign in front of the radical and S_2 to the minus sign. Finally, from $c_{\theta_t'}^2 = 1 - s_{\theta_t'}^2$, we get

$$c_{\theta_t'}^2 = \frac{(2M_2'' + M_1'') \mp \left(M_1''^2 - 4M_2''L_1''^2\right)^{\frac{1}{2}}}{2M_2''} = (S_4, S_3) \quad (74)$$

$$c_{\theta_t'} = \pm(S_4)^{\frac{1}{2}} \quad (75)$$

$$c_{\theta_t'} = \pm(S_3)^{\frac{1}{2}} \quad (76)$$

The S_4 solution corresponds to the minus sign in Eq. (74) and S_3 to the plus sign. Starting from $\tau_c = 0$ deg, the radical in Eqs. (71) and (74) is evaluated to find out whether it is positive or negative. If it is negative, no solution is possible, and therefore τ_c is increased and the test carried out once more until it satisfies the positive semidefinite property. Then the four solutions of interest are obtained from

$$\theta_t' = \tan^{-1}\left[\frac{(S_1)^{\frac{1}{2}}}{-(S_4)^{\frac{1}{2}}}\right] \quad (77)$$

$$\theta_t' = \tan^{-1}\left[\frac{-(S_1)^{\frac{1}{2}}}{(S_4)^{\frac{1}{2}}}\right] \quad (78)$$

$$\theta_t' = \tan^{-1}\left[\frac{(S_2)^{\frac{1}{2}}}{(S_3)^{\frac{1}{2}}}\right] \quad (79)$$

$$\theta_t' = \tan^{-1}\left[\frac{-(S_2)^{\frac{1}{2}}}{-(S_3)^{\frac{1}{2}}}\right] \quad (80)$$

after which the corresponding θ_t'' solutions are obtained from Eqs. (66) and (67). Then Δa is evaluated from Eq. (63), and both Δe_x and Δe_y are computed from Eqs. (64) and (65) to make sure that they both vanish. The solutions in Eqs. (77) and (80) provide negative Δa strategies, whereas their mirror solutions obtained from Eqs. (78) and (79), respectively, provide equal but positive Δa values. The largest Δa changes being of interest, they are found to correspond to Eq. (79) for $\Delta a > 0$ and Eq. (80) for $\Delta a < 0$. As τ_c is increased, the largest Δa change is reached when $\tau_c = \tau_f/2$, meaning that the optimal switch point is located at the midpoint of the sunlit arc OO′. Let $\tau_f = 280$ deg, $a_0 = 10{,}000$ km, $\mu = 398{,}601.3$ km^3/s^2, and $k = 3.5 \times 10^{-7}$ km/s^2. Starting from $\tau_c = 10$ deg and in 10-deg increments thereafter, the radical in Eq. (71) is found to be negative until $\tau_c = 80$ deg. Next, the four solutions for θ_t' in Eqs. (77–80) are evaluated, followed by the four corresponding angles θ_t''. Finally, Δa, Δe_x, and Δe_y corresponding to each of the preceding solutions are computed. As was the case for the analysis in the previous section (strategy 1), not all four solutions pass the $\Delta e_x = \Delta e_y = 0$ condition initially. After $\tau_c = 170$ deg, only the last two solutions are valid. At $\tau_c = 210$ deg, the radical fails the positive semidefinite test, and at $\tau_c = 260$ deg, it is exactly equal to zero, but all four solutions are invalid because Δe_x and Δe_y are not driven to zero (in practice 10^{-19} or less). The reason for this is that we have not enforced either the $M_1'' < 0$ condition as in the second section or the more relevant condition $s_{\theta_t'}^2 < 1$, which would have eliminated all the invalid solutions. Nonetheless, the numerical scheme derived earlier is simple enough so that there is no need for the enforcement of additional conditions. At $\tau_c = 140$ deg, the largest $\Delta a = 6.938$ km is achieved with $\theta_t' = 36.05$ deg and $\theta_t'' = -36.05$ deg.

It is then seen that, when $\tau_c = \tau_f/2$, the pitch angles are equal in magnitude but opposite in sign. As was conjectured in the analysis of the second section, the other solution that satisfies $\Delta e_x = \Delta e_y = 0$ and provides the smaller $\Delta a > 0$ value is obtained with $\theta_t' = 100.31$ deg and $\theta_t'' = 79.68$ deg for the same $\tau_c = 140$ deg providing a Δa of 0 km in this case. This type of solution almost always involves a deceleration leg, whereas the Δa maximizing solutions are always either accelerating or decelerating, depending on

Table 1 Relative performance of strategies 1 and 2 (parentheses indicate strategy 1)

a, km	7,000	10,000	20,000	30,000	40,000
τ_f, deg	220	280	322	335	341
$\Delta a_{\max}$, km	2.31	8.58	78.9	277	669
δ, deg	140	80	38	25	19
(τ_1), deg	(20)	(50)	(70)	(77)	(80)
θ_t', deg	54	36	18	12	9.4
θ_t'', deg	−54	−36	−18	−12	−9.4
Δa, km	1.34	6.93	74.8	270	659
	(1.18)	(6.56)	(71.3)	(263)	(639)
$\Delta a/\Delta a_{\max}$, %	58	71	80	97	98
λ	5,823.049823	8,379.265958	13,034.177567	14,569.241955	15,548.465162
Δa (opt.), km	2.107	7.660	75.856	272.102	661.563
$\Delta a/\Delta a_{\text{opt}}$, %	63	90	98.6	99.2	99.6

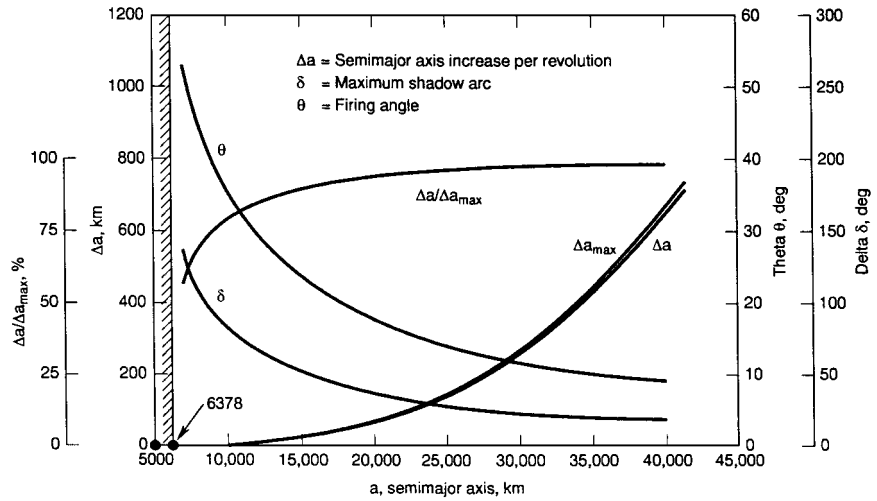

Fig. 7 Relative performance characteristics vs orbit semimajor axis.

whether $\Delta a > 0$ or $\Delta a < 0$ is desired. Finally, in Fig. 7, the results of a series of runs for various circular orbits from LEO to geosynchronous Earth orbit are depicted for the worst case of shadowing, which takes place when the sun–Earth line is contained in the spacecraft orbit plane. The total maximum shadow angle δ in this case is obtained simply from

$$\delta = \pi - 2\cos^{-1}(R/a) \tag{81}$$

where R is the Earth's radius. Then

$$\tau_f = \pi + 2\cos^{-1}(R/a) \tag{82}$$

and the Δa maximizing switch point

$$\tau_c = (\pi/2) + \cos^{-1}(R/a) \tag{83}$$

Table 1 and Fig. 7 show, as a function of the semimajor axis, the corresponding values of τ_f, $\Delta a_{\max}$ (obtained through tangential thrusting with corresponding eccentricity buildup), δ, as well as τ_1 of the preceding section and strategy, and finally $\theta = |\theta_t'| = |\theta_t''|$, Δa [from Eq. (63)], and $\Delta a/\Delta a_{\max}$. The numbers in parentheses in Table 1 are for τ_1 and the maximizing Δa from strategy 1. It is clear that, as the shadow arc gets smaller with altitude, the pitch angle decreases accordingly, and the Δa achieved after one revolution of intermittent thrusting becomes comparable to the $\Delta a_{\max}$ achieved by tangential thrust, which would be by definition the absolute maximum value. It is also seen that strategy 1 is very nearly optimal because it provides Δa values slightly less than the optimal values possible with strategy 2. Letting α now represent the thrust acceleration pitch angle measured from the radial direction, the optimal α profile that maximizes Δa while constraining Δe at zero can also be determined. The variation of parameters equations in terms of f_r and f_θ for the general elliptic case that are written as

$$\dot{a} = (2a^2/h)[es_{\theta^*} f_r + (p/r) f_\theta]$$

$$\dot{e} = (1/h)\{ps_{\theta^*} f_r + [(p+r)c_{\theta^*} + re] f_\theta\}$$

can also be cast as[3]

$$\dot{a} = \frac{2es_{\theta^*}}{n(1-e^2)^{\frac{1}{2}}} f_r + \frac{2(1+ec_{\theta^*})}{n(1-e^2)^{\frac{1}{2}}} f_\theta \tag{84}$$

$$\dot{e} = \frac{(1-e^2)^{\frac{1}{2}} s_{\theta^*}}{na} f_r + \frac{(1-e^2)^{\frac{1}{2}}}{nae}\left[1 + ec_{\theta^*} - \frac{1-e^2}{1+ec_{\theta^*}}\right] f_\theta \tag{85}$$

Measuring θ^* from the shadow exit point and setting $e = 0$ in the preceding two equations results in

$$\dot{a} = 2f_\theta/n \tag{86}$$

$$\dot{e} = (s_{\theta^*}/na) f_r + (2c_{\theta^*}/na) f_\theta \tag{87}$$

which are further reduced by using $f_r = kc_\alpha$ and $f_\theta = ks_\alpha$ and by integrating between 0 and τ_f (Fig. 6), yielding the changes in a and e as in[3]

$$\Delta a = \frac{2ka^3}{\mu} \int_0^{\tau_f} s_\alpha \, \mathrm{d}\theta^* \tag{88}$$

$$\Delta e = \frac{ka^2}{\mu} \int_0^{\tau_f} (c_\alpha s_{\theta^*} + 2s_\alpha c_{\theta^*}) \, \mathrm{d}\theta^* \tag{89}$$

The maximization of Δa subject to $\Delta e = 0$ leads to the adoption of the following performance index with λ, the Lagrange multiplier for the $\Delta e = 0$ constraint:

$$I(\alpha) = \int_0^{\tau_f} \frac{2ka^3}{\mu} s_\alpha \, \mathrm{d}\theta^* + \lambda \left[\int_0^{\tau_f} \frac{ka^2}{\mu} (c_\alpha s_{\theta^*} + 2s_\alpha c_{\theta^*}) \, \mathrm{d}\theta^* \right]$$

$$I(\alpha) = \int_0^{\tau_f} \left\{ \frac{ka^2}{\mu} [2as_\alpha + \lambda_1 (c_\alpha s_{\theta^*} + 2s_\alpha c_{\theta^*})] \right\} \mathrm{d}\theta^* \tag{90}$$

The optimal control law for α is obtained from Euler's equation, which reduces to $\partial F/\partial\alpha = 0$, where F is the integrand in Eq. (90), resulting in

$$\tan\alpha = \frac{2(a + \lambda c_{\theta^*})}{\lambda s_{\theta^*}} \tag{91}$$

such that

$$s_\alpha^2 = \frac{4(a + \lambda c_{\theta^*})^2}{\lambda^2 s_{\theta^*}^2 + 4(a + \lambda c_{\theta^*})^2}, \qquad c_\alpha^2 = \frac{\lambda^2 s_{\theta^*}^2}{\lambda^2 s_{\theta^*}^2 + 4(a + \lambda c_{\theta^*})^2}$$

Substituting in Eq. (89) results in

$$\Delta e = \frac{ka^2}{\mu}\int_0^{\tau_f} \frac{\left(4ac_{\theta^*} + \lambda + 3\lambda c_{\theta^*}^2\right)}{\left[4a^2 + 4a\lambda c_{\theta^*} + \lambda\left(\lambda + 3\lambda c_{\theta^*}^2 + 4ac_{\theta^*}\right)\right]^{\frac{1}{2}}} \mathrm{d}\theta^* = 0 \tag{92}$$

The value of λ is determined numerically by performing a 10-point Gauss–Legendre quadrature of the preceding integral and by searching on λ to establish the zero crossing of the Δe function, after which the Wijngaarden–Dekker–Brent method, which combines root bracketing, bisection, and inverse quadratic interpolation, is applied to converge on the exact value of λ from the neighborhood of the zero crossing. Once λ is thus determined, s_α and c_α are readily obtained from the control law in Eq. (91), and the change Δa in Eq. (88) is evaluated also by numerical quadrature. The last three columns of Table 1 show for the same $k = 3.5\times10^{-7}$ km/s^2 constant acceleration the achieved optimal Δa for the five orbit radii with maximum shadowing. As expected, Δa_{opt} falls between the values of $\Delta a_{\max}$ for pure tangential thrusting and Δa of strategy 2 of this present paper. Constraining the eccentricity at the zero value, even in the worst case of maximum shadowing, results in a loss of only 10% in achieved Δa with respect to the unconstrained tangential thrust case in LEO and negligible loss in higher orbit. The purely analytic scheme using piecewise constant pitch profiles is also very effective in orbit raising, being less effective only in low orbit as shown in Table 1.

Concluding Remarks

Two coplanar orbit-raising strategies with near-optimal performance have been analyzed. The orbit is kept circular during the transfer even though thrusting is intermittent due to the presence of Earth shadow. It is better from a practical point of view to use strategy 1 initially in LEO and to switch later to the other strategy when the period of the orbit gets larger, allowing thereby a thrust attitude reorientation maneuver to take place just before entry into shadow or immediately after exit with negligible penalty in overall performance. The solutions presented here are very easy to generate and robust inasmuch as a table of the achieved semimajor axis change vs the switch point location is established and the largest change selected by way of a search and sorting routine. These results are further compared with the optimal eccentricity constrained solutions, which require integral evaluations through numerical quadrature and Lagrange multiplier determination through numerical search, and are shown to be near optimal in LEO and almost equivalent to the optimal in higher orbit.

Acknowledgment

This work was supported by the U.S. Air Force Space and Missile Systems Center under Contract F04701-88-C-0089.

References

[1] Edelbaum, T. N., "Propulsion Requirements for Controllable Satellites," *ARS Journal*, Aug. 1961, pp. 1079–1089.

[2] Wiesel, W. E., and Alfano, S., "Optimal Many-Revolution Orbit Transfer," American Astronautical Society, AAS 83-352, Aug. 1983.

[3] Cass, J. R., "Discontinuous Low Thrust Orbit Transfer," M.S. Thesis, School of Engineering, U.S. Air Force Inst. of Technology, AFIT/GA/AA/83D-1, Wright–Patterson AFB, OH, Dec. 1983.

[4] McCann, J. M., "Optimal Launch Time for a Discontinuous Low Thrust Orbit Transfer," M.S. Thesis, School of Engineering, U.S. Air Force Inst. of Technology, AFIT/GA/AA/88D-7, Wright–Patterson AFB, OH, Dec. 1988.

[5] Dickey, M. R., Klucz, R. S., Ennix, K. A., and Matuszak, L. M., "Development of the Electric Vehicle Analyzer," Astronautics Lab., U.S. Air Force Space Technology Center, Rept. AL-TR-90-006, Edwards AFB, CA, June 1990.

[6] Kechichian, J. A., "Low-Thrust Inclination Control in the Presence of Earth Shadow," American Astronautical Society, AAS 91-157, Feb. 1991.

[7] Kechichian, J. A., "Orbit Raising with Low Thrust Tangential Acceleration in the Presence of Earth Shadow," American Astronautical Society, AAS 91-513, Aug. 1991.

[8] Kaplan, M. H., *Modern Spacecraft Dynamics and Control*, Wiley, New York, 1976, pp. 348–353.

F. H. Lutze Jr.
Associate Editor